Applied and Computational Mechanics 5 (2011) 111–122

Modal properties of the flexural vibrating package of rods linked by spacer grids

V. Zeman[a,*], Z. Hlaváč[a]

[a] *Faculty of Applied Sciences, University of West Bohemia, Univerzitní 22, 306 14 Plzeň, Czech Republic*

Received 29 September 2010; received in revised form 23 March 2011

Abstract

The paper deals with the modelling and modal analysis of the large package of identical parallel rods linked by transverse springs (spacer grids) placed on several level spacings. The rod discretization by finite element method is based on Rayleigh beam theory. For the cyclic and central symmetric package of rods (such as fuel rods in nuclear fuel assembly) the system decomposition on the identical revolved rod segments was applied. A modal synthesis method with condensation is used for modelling of the whole system. The presented method is the first step for modelling the nuclear fuel assembly vibration caused by excitation determined by the support plate motion of the reactor core.

Keywords: package of rods, spacer grids, modelling of vibration, modal values, modal synthesis method

1. Introduction

Dynamic properties of nuclear fuel assembly (FA) are usually investigated using global models, whose properties are gained experimentally, as it was shown e.g. in [3, 6] and in several research reports elaborated mainly in OKB Gidropress Podolsk in Russia. Experimentally gained eigenfrequencies and eigenvectors serve as initial data for parametric identification of the American nuclear VVANTAGE6 FA [7] and Russian TVSA-T FA in nuclear power plant (NPP) Temelín [1]. These models, however, do not enable investigation of dynamic deformations and load of FA components, such as the fuel rods, guide thimbles, angle pieces, spacer grids and other.

Nuclear fuel assemblies are in term of mechanics very complicated systems of beamed type, whose basic structure is formed from large number of parallel rods linked by transverse spacer grids (Fig. 1). The spacer grids inside the every segment (gray) are shown by solid lines and within the segments by dashed lines. All springs at the level of one spacer grid are the same ones. All the rods are identical including boundary conditions. The goal of the paper is a development of analytical method for modelling and modal analysis of large package of parallel rods linked by spacer grids placed on several transverse planes.The variable modifying mathematical model of this large system will be in future used for modelling the nuclear FA vibration caused by pressure pulsations [9] and seismic excitation [1] in terms of fuel rods deformation and abrasion of fuel element coating [4]. The developed methodology and software can be used for vibration analysis of the different large parallel beam systems.

*Corresponding author. Tel.: +420 377 632 332, e-mail: zemanv@kme.zcu.cz.

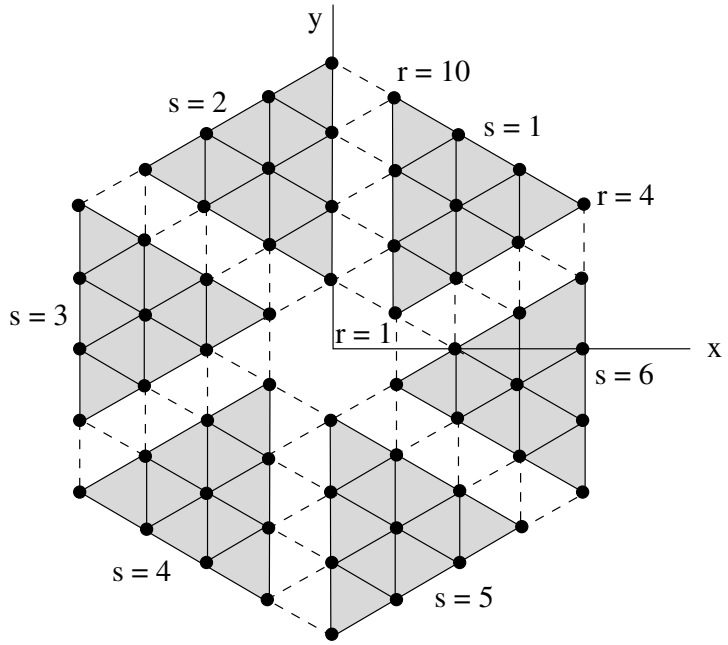

Fig. 1. The rod package cross-section with six segments linked by spacer grids

2. Mathematical model of the system

2.1. Modelling of the rod

The creation of a model is divided into three steps. The *first step* is the modelling of one isolated rod r in the segment s (see segment $s = 1$ in Fig. 2) by means of 1D beam finite elements [5] in the coordinate system

$$\boldsymbol{q}_{r,s} = [\ldots, \xi_{r,g}^{(s)}, \eta_{r,g}^{(s)}, \vartheta_{r,g}^{(s)}, \psi_{r,g}^{(s)}, \ldots]^T, \quad g = 1, \ldots, G, \tag{1}$$

where $\xi_{r,g}^{(s)}, \eta_{r,g}^{(s)}$ are mutually perpendicular lateral displacements and $\vartheta_{r,g}^{(s)}, \psi_{r,g}^{(s)}$ are bending angles of rod cross-section in contact nodal point g on the level of grid g (in Fig. 3 $g = 1, 2, 3$). The directions of $\xi_{r,g}^{(s)}$ displacements are radial with respect to vertical axis of the package (nuclear fuel assembly).

The detailed model of the rod created by FEM is replaced by alternate rod devided into $G + 1$ prismatic beam elements in contact nodal points with grids. Every beam element is determined by parameters ρ (mass density), A (cross-section area), J (second moment of the cross-section area), l (length) and E (Young's modulus) for concrete material. Mathematical model of the beam element of the alternate rod in coordinate system with different displacement arrangement in comparison with (1)

$$\boldsymbol{q}_{r,s}^{*} = [\ldots, \xi_{r,g}^{(s)}, \psi_{r,g}^{(s)}, \eta_{r,g}^{(s)}, \vartheta_{r,g}^{(s)}, \ldots]^T, \quad g = 1, \ldots, G, \tag{2}$$

which is more suitable for the beam element modelling, has the form [5]

$$\boldsymbol{M}_e^{*} = \begin{bmatrix} \boldsymbol{S}_1^{-T}(\boldsymbol{I}_1 + \boldsymbol{I}_2)\boldsymbol{S}_1^{-1} & \boldsymbol{0} \\ \boldsymbol{0} & \boldsymbol{S}_2^{-T}(\boldsymbol{I}_1 + \boldsymbol{I}_2)\boldsymbol{S}_2^{-1} \end{bmatrix}; \boldsymbol{K}_e^{*} = \begin{bmatrix} \boldsymbol{S}_1^{-T}\boldsymbol{I}_3\boldsymbol{S}_1^{-1} & \boldsymbol{0} \\ \boldsymbol{0} & \boldsymbol{S}_2^{-T}\boldsymbol{I}_3\boldsymbol{S}_2^{-1} \end{bmatrix}, \tag{3}$$

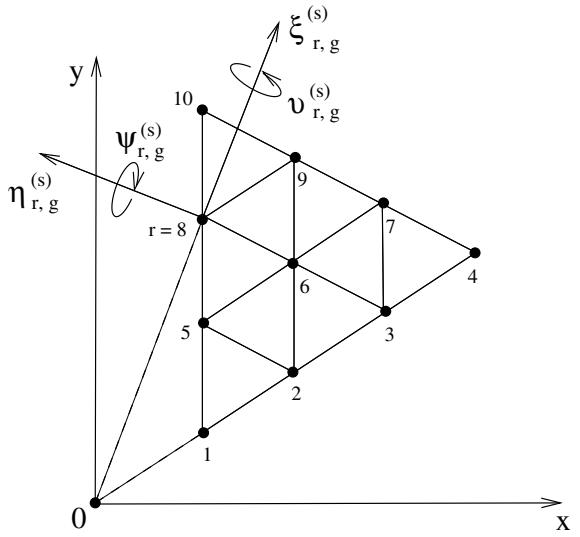

Fig. 2. Displacements of rod r of segment $s = 1$ in contact points with spacer grid g

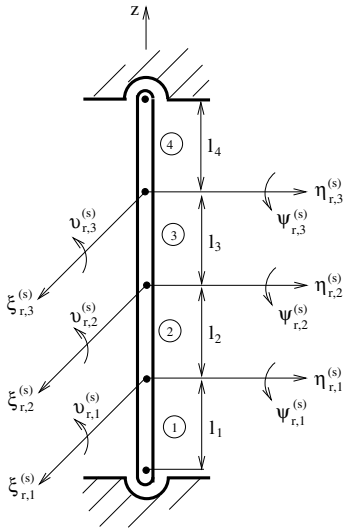

Fig. 3. The displacements of rod r in segment s at the level of spacer grids

where

$$\boldsymbol{I}_1 = \rho A l \begin{bmatrix} 1 & \frac{l}{2} & \frac{l^2}{3} & \frac{l^3}{4} \\ \frac{l}{2} & \frac{l^2}{3} & \frac{l^3}{4} & \frac{l^4}{5} \\ \frac{l^2}{3} & \frac{l^3}{4} & \frac{l^4}{5} & \frac{l^5}{6} \\ \frac{l^3}{4} & \frac{l^4}{5} & \frac{l^5}{6} & \frac{l^6}{7} \end{bmatrix}, \quad \boldsymbol{I}_2 = \rho J l \begin{bmatrix} 0 & 0 & 0 & 0 \\ 0 & 1 & l & l^2 \\ 0 & l & \frac{4l^2}{3} & \frac{3l^3}{2} \\ 0 & l^2 & \frac{3l^3}{2} & \frac{9l^4}{5} \end{bmatrix},$$

$$\boldsymbol{I}_3 = EJl \begin{bmatrix} 0 & 0 & 0 & 0 \\ 0 & 0 & 0 & 0 \\ 0 & 0 & 4 & 6l \\ 0 & 0 & 6l & 12l^2 \end{bmatrix}, \quad \boldsymbol{S}_1 = \begin{bmatrix} 1 & 0 & 0 & 0 \\ 0 & 1 & 0 & 0 \\ 1 & l & l^2 & l^3 \\ 0 & 1 & 2l & 3l^2 \end{bmatrix}, \quad \boldsymbol{S}_2 = \begin{bmatrix} 1 & 0 & 0 & 0 \\ 0 & -1 & 0 & 0 \\ 1 & l & l^2 & l^3 \\ 0 & -1 & -2l & -3l^2 \end{bmatrix}.$$

For model transposition into general coordinates $\boldsymbol{q}_{r,s}$ defined in (1) mass and stiffness matrices must be transformed in the form

$$\boldsymbol{X}_e = \boldsymbol{P}^T \boldsymbol{X}_e^* \boldsymbol{P}, \quad \boldsymbol{X} = \boldsymbol{M}, \boldsymbol{K}, \tag{4}$$

where permutation matrix is

$$\boldsymbol{P} = \begin{bmatrix} 1 & 0 & 0 & 0 & 0 & 0 & 0 & 0 \\ 0 & 0 & 0 & 1 & 0 & 0 & 0 & 0 \\ 0 & 0 & 0 & 0 & 1 & 0 & 0 & 0 \\ 0 & 0 & 0 & 0 & 0 & 0 & 0 & 1 \\ 0 & 1 & 0 & 0 & 0 & 0 & 0 & 0 \\ 0 & 0 & 1 & 0 & 0 & 0 & 0 & 0 \\ 0 & 0 & 0 & 0 & 0 & 1 & 0 & 0 \\ 0 & 0 & 0 & 0 & 0 & 0 & 1 & 0 \end{bmatrix}.$$

By FE summation we get the mass and stiffness matrices of the alternative rod (subscript R) in the block diagonal form

$$\boldsymbol{X}_R = [x_{ij}^{(R)}] = \sum_{e=1}^{G+1} \mathrm{diag}\,[\boldsymbol{0}, \boldsymbol{X}_e, \boldsymbol{0}], \quad \boldsymbol{X} = \boldsymbol{M}, \boldsymbol{K}, \quad x = m, k, \tag{5}$$

with block matrices $\boldsymbol{X}_e$ determined in (4). Matrices in (5) must be arranged in accordance with boundary conditions. The modal behaviour of the conservative mathematical model of the alternate rod is determined by the matrix equation of motion

$$\boldsymbol{M}_R\ddot{\boldsymbol{q}}_{r,s} + \boldsymbol{K}_R\boldsymbol{q}_{r,s} = \boldsymbol{0}. \tag{6}$$

Eigenfrequencies Ω_ν and eigenvectors $\boldsymbol{v}_\nu$ of one isolated alternate rod depend on global material parameters ρ, E and local geometrical parameters A_e, $J_e\,(e = 1, \ldots, G+1)$ of the beam elements. The aim of tuning of the mathematical model (6) is to change the values of the above-mentioned parameters to new values to achieve required modal values. Global material and local geometrical parameters, that will be changed, constitute a vector of tuning parameters $\boldsymbol{p} = [p_j]$. The selected tuned modal values — eigenfrequencies and eigenvectors coordinates — form the vector of tuning $\boldsymbol{l} = [\ldots, \Omega_\nu, \ldots, \boldsymbol{v}_\nu, \ldots]^T$ and the desired vector of tuning $\boldsymbol{l}^* = [\ldots, \Omega^*_\nu, \ldots, \boldsymbol{v}^*_\nu, \ldots]^T$, where Ω^*_ν and $\boldsymbol{v}^*_\nu$ are eigenfrequencies and eigenvectors calculated from the detailed finite element model or experimentally obtained. The tuning problem of the alternate rod model can be formulated as an optimization problem with the objective function

$$\psi(\boldsymbol{p}) = \sum_i g_i \left[1 - \frac{l_i(\boldsymbol{p})}{l^*_i}\right], \tag{7}$$

where g_i is a weighted coefficient corresponding to i-th coordinate of vectors $\boldsymbol{l}(\boldsymbol{p})$ and $\boldsymbol{l}^*$. The tuning parameters are constrained by lower and upper limits

$$\boldsymbol{p}_L \le \boldsymbol{p} \le \boldsymbol{p}_U. \tag{8}$$

2.2. Modelling of the rod segment

The *second step* is the modelling of the rod segment s (see segment $s = 1$ in Fig. 1) in which the rods are linked by transverse springs with small prestressing placed on several level spacings $g = 1, \ldots, G$. The stiffnesses k_g of the springs in one lateral horizontal plane are identical. The generalized coordinates of the segment s are

$$\boldsymbol{q}_s = [\boldsymbol{q}^T_{1,s}, \boldsymbol{q}^T_{2,s}, \ldots, \boldsymbol{q}^T_{r,s}, \ldots, \boldsymbol{q}^T_{R,s}]^T, \tag{9}$$

where R is number of the rods in the segment. The deformation $d^{(s)}_{q,g}$ of the spring k_g between two rods u and v of the segment s (see Fig. 4), modelling the coupling q by means of spacer grid g, is

$$d^{(s)}_{q,g} = \xi^{(s)}_{v,g}\cos\gamma_q + \eta^{(s)}_{v,g}\sin\gamma_q + \xi^{(s)}_{u,g}\cos\beta_q - \eta^{(s)}_{u,g}\sin\beta_q\,. \tag{10}$$

The stiffness matrix $\boldsymbol{K}_{qg}$ corresponding to this coupling results from identity

$$\frac{\partial E^{(s)}_{q,g}}{\partial \boldsymbol{q}_s} = \boldsymbol{K}_{qg}\boldsymbol{q}_s\,, \tag{11}$$

where $E^{(s)}_{q,g} = \frac{1}{2}k_g(d^{(s)}_{q,g})^2$ is potential (deformation) energy of latter coupling. This matrix has the form

$$\boldsymbol{K}_{qg} = k_g \begin{bmatrix} & \vdots & & \vdots & \\ \cdots & \boldsymbol{A}_q & \cdots & \boldsymbol{B}_q & \cdots \\ & \vdots & & \vdots & \\ \cdots & \boldsymbol{B}^T_q & \cdots & \boldsymbol{C}_q & \cdots \\ & \vdots & & \vdots & \end{bmatrix}, \quad g = 1, \ldots, G\,, \quad q = 1, \ldots, Q\,, \tag{12}$$

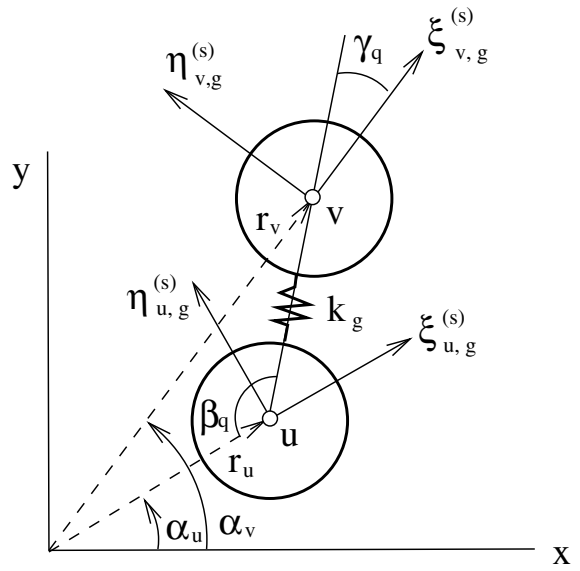

Fig. 4. The spring between two rods replacing the stiffness of the spacer grid g

where

$$\boldsymbol{A}_q = \begin{bmatrix} \cos^2\beta_q & -\sin\beta_q\cos\beta_q \\ -\sin\beta_q\cos\beta_q & \sin^2\beta_q \end{bmatrix}, \quad \boldsymbol{B}_q = \begin{bmatrix} \cos\beta_q\cos\gamma_q & \sin\gamma_q\cos\beta_q \\ -\sin\beta_q\cos\gamma_q & -\sin\beta_q\sin\gamma_q \end{bmatrix},$$

$$\boldsymbol{C}_q = \begin{bmatrix} \cos^2\gamma_q & \sin\gamma_q\cos\gamma_q \\ \sin\gamma_q\cos\gamma_q & \sin^2\gamma_q \end{bmatrix} \tag{13}$$

and angles β_q, γ_q (see Fig. 4) are determined by polar coordinates $r_u,\ \alpha_u$ and $r_v,\ \alpha_v$ of the linked rods [2]. The blocks $\boldsymbol{A}_q,\ \boldsymbol{B}_q,\ \boldsymbol{C}_q$ in (12) are localized at positions corresponding to coordinates $\xi^{(s)}_{v,g}, \eta^{(s)}_{v,g}$ and $\xi^{(s)}_{u,g}, \eta^{(s)}_{u,g}$ in the vector of generalized coordinates $\boldsymbol{q}_s$ in (9). The conservative mathematical model of the arbitrary rod segment s is

$$\boldsymbol{M}_s\ddot{\boldsymbol{q}}_s + (\boldsymbol{K}_s + \sum_{q=1}^{Q}\sum_{g=1}^{G}\boldsymbol{K}_{qg})\boldsymbol{q}_s = \boldsymbol{0}\,, \quad s = 1,\ldots,S\,, \tag{14}$$

where Q is the number of the transverse springs inside one segment. The mass $\boldsymbol{M}_s$ and stiffness $\boldsymbol{K}_s$ matrices of the all identical parallel uncoupled identified rods in the segment are block diagonal

$$\boldsymbol{X}_s = \mathrm{diag}\,[\boldsymbol{X}_R,\ldots,\boldsymbol{X}_R]\,, \quad \boldsymbol{X} = \boldsymbol{M},\boldsymbol{K}\,. \tag{15}$$

2.3. Modelling of the rod segment package

The *third* and *final step* is the rod segment package model assembly (below system), that contains the number of S identical revolved rod segments linked by transverse springs between outer rods (in Fig. 1 marked with dashed line). The mass and stiffness matrices of the segments (see Eq. (14)) modelled in radial and circumferential displacements of rod nodal points are identical. Therefore the conservative model of the system in the configuration space

$$\boldsymbol{q} = [\boldsymbol{q}_1^T,\ldots,\boldsymbol{q}_s^T,\ldots,\boldsymbol{q}_S^T]^T \tag{16}$$

can be written as

$$\boldsymbol{M}\ddot{\boldsymbol{q}} + (\boldsymbol{K} + \boldsymbol{K}_C)\boldsymbol{q} = \boldsymbol{0}\,, \tag{17}$$

where mass $\boldsymbol{M}$ and stiffness $\boldsymbol{K}$ matrices of the mutually isolated segment package are block diagonal matrices

$$\boldsymbol{M} = \mathrm{diag}\left[\boldsymbol{M}_S, \ldots, \boldsymbol{M}_S\right], \quad \boldsymbol{K} = \mathrm{diag}\left[\boldsymbol{K}_S^*, \ldots, \boldsymbol{K}_S^*\right], \tag{18}$$

where

$$\boldsymbol{K}_S^* = \boldsymbol{K}_S + \sum_{q=1}^{Q} \sum_{g=1}^{G} \boldsymbol{K}_{qg}\,.$$

The number of the block matrices $\boldsymbol{M}_S$ and $\boldsymbol{K}_S^*$ in global matrices $\boldsymbol{M}$, $\boldsymbol{K}$ corresponds to number of segments. The structure of the coupling matrix $\boldsymbol{K}_C$ between segments is analogical to the coupling matrix between rods inside the segment.

2.4. Condensed model of the system

The global model (17) has too large DOF number $n = 4RGS$ for calculation of the dynamic response excited by different sources of excitation. Therefore we compile the condensed model of the large package of rods using the modal synthesis method [5]. After the modal analysis of one isolated rod segment with $n_S = 4RG$ number of DOF we choose a set of its m_S master eigenvectors normed by M-norm which will be arranged in modal submatrix ${}^m\boldsymbol{V}_S \in R^{n_S,m_S}$ corresponding to spectral submatrix ${}^m\boldsymbol{\Lambda}_S \in R^{m_S,m_S}$. A set of other eigenmodes of each segment will be neglected. We introduce the transformation of rod segment generalized coordinates

$$\boldsymbol{q}_s = {}^m\boldsymbol{V}_S \boldsymbol{x}_s\,, \quad s = 1, \ldots, S\,. \tag{19}$$

The condensed mathematical model of the system has the form [5]

$$\ddot{\boldsymbol{x}} + ({}^m\boldsymbol{\Lambda} + {}^m\boldsymbol{V}^T \cdot \boldsymbol{K}_C \cdot {}^m\boldsymbol{V})\boldsymbol{x} = \boldsymbol{0}\,, \tag{20}$$

where $\boldsymbol{x} = [\boldsymbol{x}_1^T, \ldots, \boldsymbol{x}_s^T, \ldots, \boldsymbol{x}_S^T]^T$ and

$${}^m\boldsymbol{\Lambda} = \mathrm{diag}\left[{}^m\boldsymbol{\Lambda}_s\right] \in R^{m,m}\,, \quad {}^m\boldsymbol{V} = \mathrm{diag}\left[{}^m\boldsymbol{V}_s\right] \in R^{n,m}\,, \quad s = 1, \ldots, S$$

are block diagonal matrices, whereas ${}^m\boldsymbol{\Lambda}_s = {}^m\boldsymbol{\Lambda}_S$, ${}^m\boldsymbol{V}_s = {}^m\boldsymbol{V}_S$ are spectral and modal submatrices of the isolated rod segment (14). Eigenfrequencies Ω_ν and eigenvectors

$$\boldsymbol{x}_\nu = [\boldsymbol{x}_{1,\nu}^T, \ldots, \boldsymbol{x}_{s,\nu}^T, \ldots, \boldsymbol{x}_{S,\nu}^T]^T\,, \quad \nu = 1, \ldots, m$$

of the system are obtained from the modal analysis of the condensed model (20). Subvectors $\boldsymbol{x}_{s,\nu}$, corresponding to rod segment s ($s = 1, \ldots, S$), can be transformed according to (19) from the space of master modal coordinates of the condensed model (20) to the original configuration space of the generalized coordinates of rod segments by

$$\boldsymbol{q}_\nu = {}^m\boldsymbol{V}\boldsymbol{x}_\nu \quad \text{or} \quad \boldsymbol{q}_\nu^{(s)} = {}^m\boldsymbol{V}_S\boldsymbol{x}_{s,\nu}\,, \quad s = 1, \ldots, S\,. \tag{21}$$

The eigenvalues calculated using the condensed model (20) are tested with respect to noncondensed model (17) for different number m_S of applied rod segment master eigenvectors on the basis of the cumulative relative error of the eigenfrequencies and the normalized cross orthogonality matrix [8].

3. Example

Let us consider the central symmetric package of rods with six rod segments (Fig. 5) linked by three identical spacer grids uniformly located between fixed ends of rods ($l_e = 1\,\mathrm{m}$, $e = 1, \ldots, 4$, see Fig. 3). Each segment has ten lines of rods and consists of $R = 55$ identical rods with fully restrained ends in the form of steel tube ($\rho = 7800\,\mathrm{kgm}^{-3}$, $E = 2 \cdot 10^{11}\,\mathrm{Pa}$) with outer radius 4.55 mm and inner radius 4.25 mm. The rod spacing is 13 mm. Eigenfrequencies f [Hz] of one *isolated rod* (without grid springs) are presented in Table 1. The eigenfrequencies of the isolated axially symmetric rod are double-frequencies.

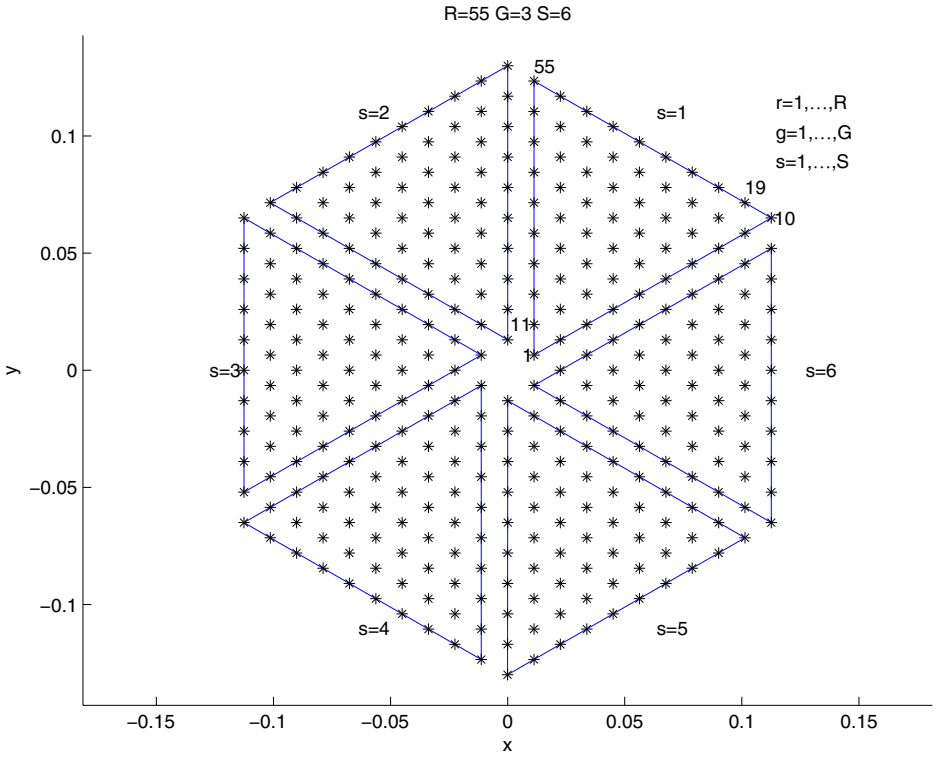

Fig. 5. The cross-section of the system with six rod segments and ten rods inline in one segment

Table 1. Rod eigenfrequencies

ν	1.2	3.4	5.6	7.8	9.10	11.12
f_ν^R	3.513	9.76	19,361	36.627	60.546	97.436

Let use consider the *isolated first rod segment* with spacer grids characterized by two different transverse springs $k_g = 100$ and $k_g = 200$ N/m for $g = 1, 2, 3$ between adjacent rods. Eigenfrequencies of these rod segments are bounded bellow by triple of eigenfrequencies $f_1^S = f_2^S = f_3^S$ equal to the lowest rod eigenfrequency pair $f_1^R = f_2^R = 3.513$ Hz. Highest rod segment triple eigenfrequencies $f_{658}^S = f_{659}^S = f_{660}^S = 97.84$ Hz for $k_g = 100$ N/m and $f_{658}^S = f_{659}^S = f_{660}^S = 98.27$ Hz for $k_g = 200$ N/m only little exceed the highest rod eigenfrequency pair $f_{11}^R = f_{12}^R = 97.436$ Hz. The spacer grids influence the spectrum of eigenfrequencies between values presented in Table 1. The number of segment eigenfrequencies between lower values in Table 1 is smaller for stiffer grids and for softer grids vice versa. As an illus-

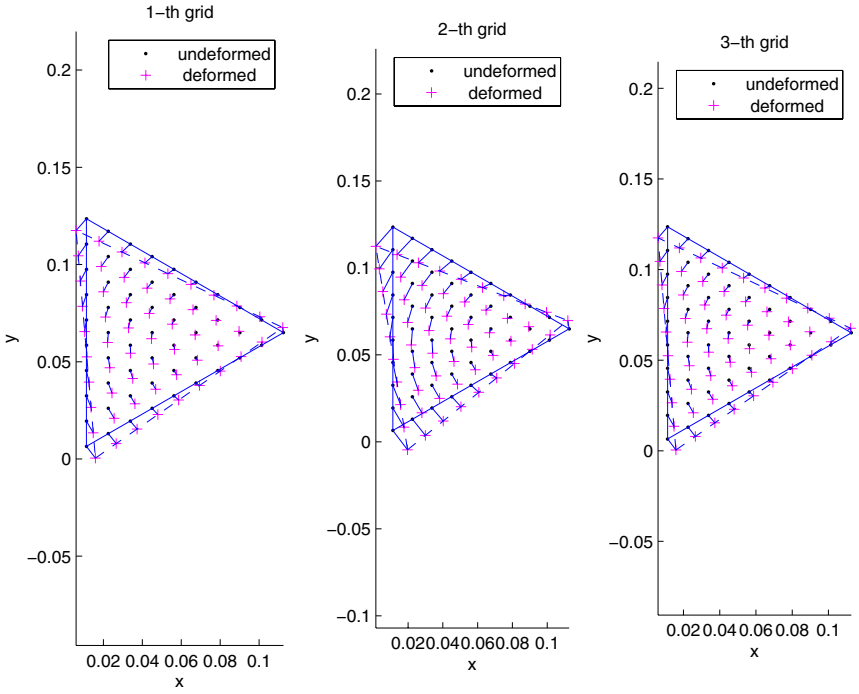

Fig. 6. The first mode shape of the spacer grids of the isolated rod segment

tration, the mode shapes of the rod segment with springs $k_g = 200$ N/m corresponding to the lowest eigenfrequency $f_1^S = 3.513$ Hz at the level of grids is shown in Fig. 6.

It follows from the figures that the spacer grids are not deformed and only transfer to new positions in consequence of different rod deformations. Analogous to the mode shapes corresponding to the first triple of eigenfrequencies, spacer grids are not deformed on mode shapes corresponding to other triples of rod segment eigenfrequencies presented in Table 1. All other eigenfrequencies and mode shapes of the rod segment from set of $n_S = 4RG = 4 \cdot 55 \cdot 3 = 660$ eigenvalues depend on spacer grid stiffnesses k_g.

The complex *package of rods* under consideration (see Fig. 5) has $n = S \cdot n_S = 3960$ DOF. The spectrum of eigenfrequencies for $k_g = 200$ N/m is distributed between values $f_1 = f_2 = f_3 = 3.513$ Hz and $f_{3958} = f_{3959} = f_{3960} = 98.334$ Hz. The lowest triple of eigenfrequencies is the same as with one segment and the highest triple of eigenfrequencies is slightly different. The spectrum is very crowded, especially for higher frequencies.

As an illustration, the mode shapes of the system at the level of the second (central) spacer grid corresponding to lowest three identical eigenfrequencies are shown in Fig. 7, 8, 9. The spacer grids are not deformed and appropriate eigenfrequencies do not depend on spacer grid stiffnesses k_g. Analogous to the isolated rod segment the mode shapes corresponding to other triples of eigenfrequencies (values are in Table 1) are characterized by transfer of undeformed spacer grids.

The condensed mathematical model (20) was applied to the calculation of eigenfrequencies $f_\nu(m_S)$ for different number of rod segment master eigenvectors m_S included in modal submatrix ${}^m\boldsymbol{V}_S$. An accuracy of condensed model was tested in terms of *relative errors* of lowest eigenfrequencies defined in the form

$$\varepsilon_\nu = \frac{|f_\nu(m_S) - f_\nu|}{f_\nu},$$

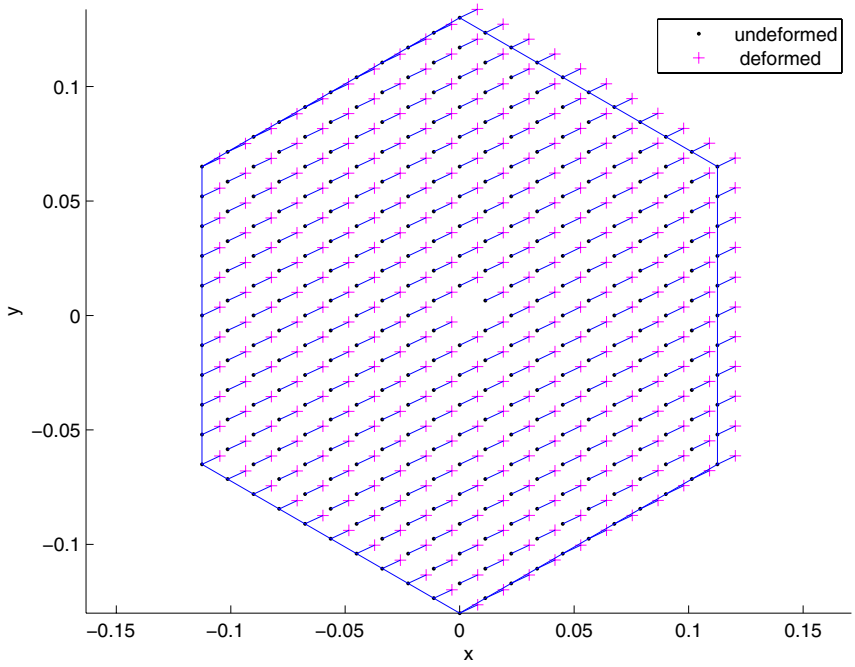

Fig. 7. The first mode shape of the second (central) spacer grid of the complex package of rods

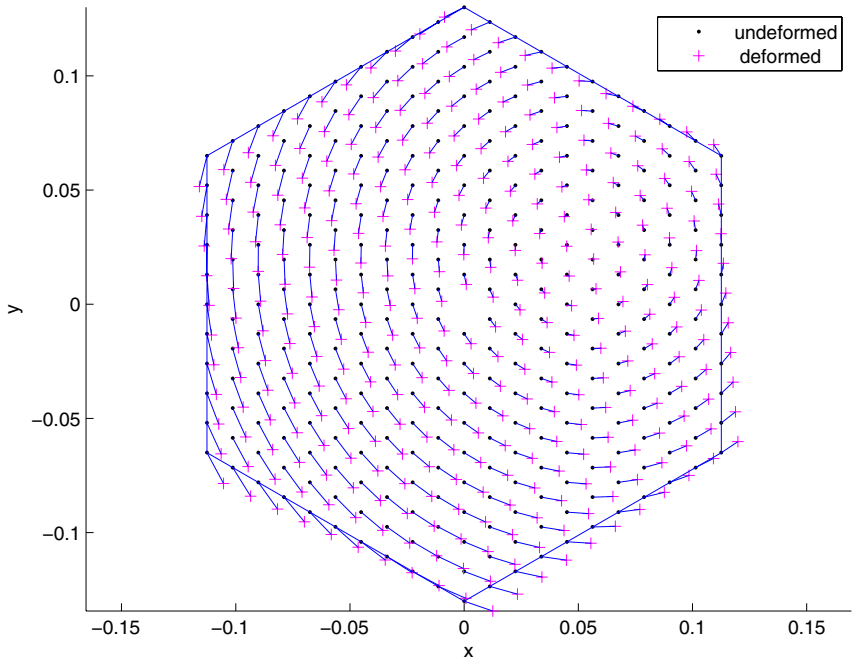

Fig. 8. The second mode shape of the second (central) spacer grid of the complex package of rods

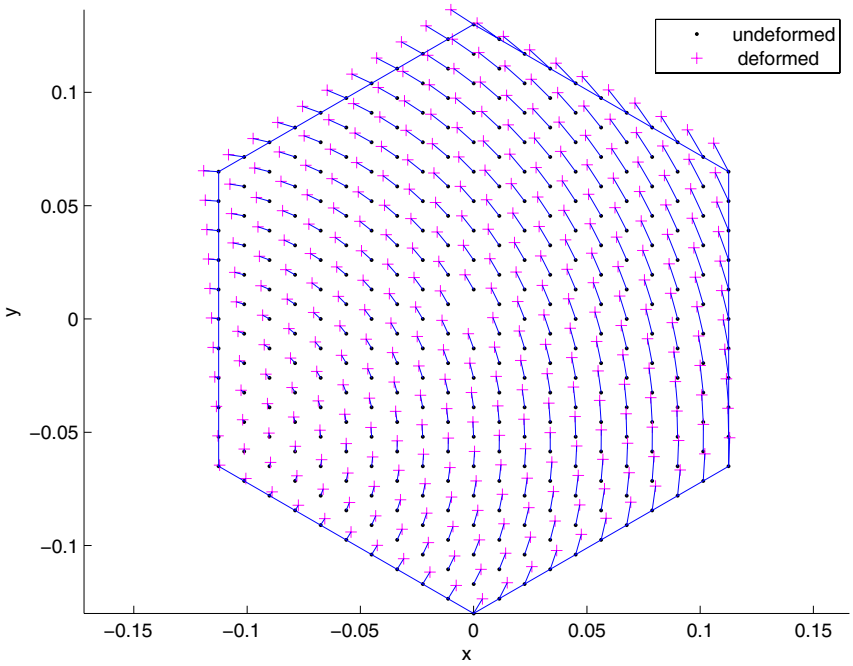

Fig. 9. The third mode shape of the second (central) spacer grid of the complex package of rods

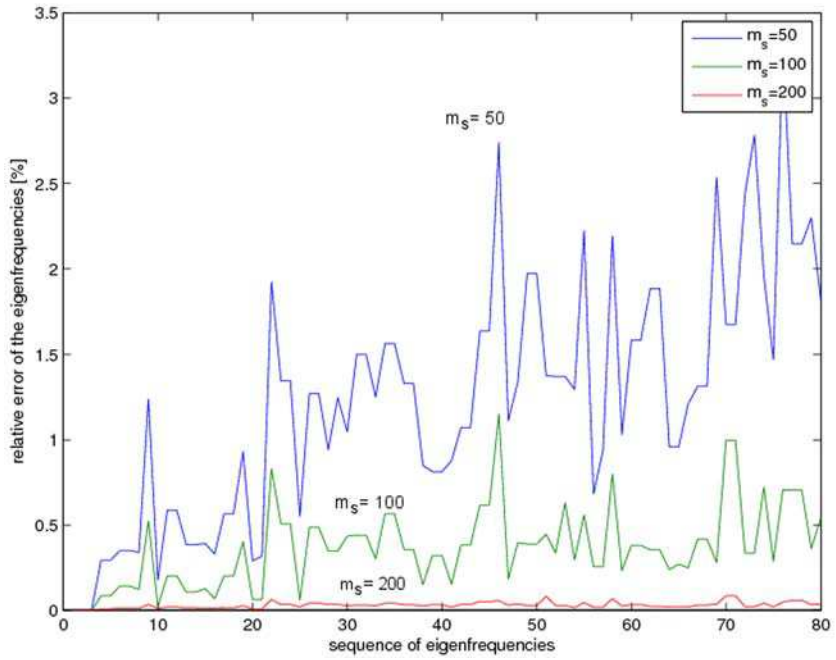

Fig. 10. The relative errors of lowest eigenfrequencies of the complex package of rods condensed model for different number of rod segment master eigenvectors m_S

where f_ν are eigenfrequencies of the full (noncondensed) model with 3960 DOF. The relative errors of 50 lowest eigenfrequencies of the condensed model for different number $m_S = 50, 100, 200$ is shown in Fig. 10. The frequency lower eigenmodes corresponding to condensed model with $m_s = 200$ segment master eigenvectors practically have no deviations from eigenmodes of the condensed model. It stands to reason that condensed model with number of DOF $m = Sm_S = 6 \cdot 200 = 1\,200$ is suitable for next phases of package rods dynamic analysis.

4. Conclusion

The described method enables to investigate effectively the flexural vibration of the large package of parallel rods linked by spacer grids. The special coordinate system of radial and orthogonal rod displacements makes possible to separate the complex package of rods into several identical revolved rod segments characterized by identical mass and stiffness matrices. This approach to modelling makes possible to significantly stream-line the computing program assemblage, modal analysis in Matlab code and to save the computer memory.

This new approach, based on the system decomposition into more rod segments and modal synthesis method with reduction of DOF number, was applied to the test package of rods which is structurally conformable to nuclear fuel assembly. In future this methodology will be used for modelling the nuclear fuel assembly vibration caused by kinematic excitation determined by the support plate motion of the reactor core.

Acknowledgements

This work was supported by the research project MSM 4977751303 of the Ministry of Education, Youth and Sports of the Czech Republic.

References

[1] Hlaváč, Z., Zeman, V., The seismic response affection of the nuclear reactor WWER1000 by nuclear fuel assemblies, Engineering Mechanics, (17) (2010) (in the press).

[2] Hlaváč, Z., Zeman, V., Flexural vibration of the package of rods linked by lattices, Proceedings of the 8-th conference Dynamic of rigid and deformable bodies 2010, Ústí nad Labem, 2010 (in Czech).

[3] Lavreňuk, P. I., Obosnovanije sovmestnosti TVSA-T PS CUZ i SVP s projektom AES Temelín, Statement from technical report TEM-GN-01, Sobstvennosť OAO TVEL (inside information of NRI Řež, 2009).

[4] Pečínka, L., Criterion assessment of fuel assemblies behaviour VV6 and TVSA-T at standard operating conditions of ETE V1000/320 type reactor, Research report DITI 300/406, NRI Řež, 2009.

[5] Slavík, J., Stejskal, V., Zeman, V., Elements of dynamics of machines, ČVUT, Praha, 1997 (in Czech).

[6] Smolík, J. and coll., VVANTAGE 6 Fuel Assembly Mechanical Test, Technical Report No. Ae 18018T, Škoda, Nuclear Machinery, Pilsen, Co. Ltd., 1995.

[7] Zeman, V., Hlaváč, Z., Pašek, M., Parametric identification of mechanical systems based on measured eigenfrequencies and mode shapes, Zeszyty naukowe nr. 8, Politechnika Slaska, Gliwice, 1998, 95–100.

[8] Zeman, V., Hajžman, M., Usage of the generalized modal synthesis method in dynamics of machines, Engineering Mechanics, 1/2 (14) (2007), 45–54.

[9] Zeman, V., Hlaváč, Z., Dynamic response of VVER1000 type reactor excited by pressure pulsations, Engineering Mechanics, 6 (15) (2008), 435–446.